The Journal of Chemical Physics

RESEARCH ARTICLE | MAY 05 2026

Role of transfer films and interfacial cracking in metallic sliding wear

Special Collection: 2026 JCP Emerging Investigators Special Collection

R. Xu ; B. N. J. Persson

Check for updates

J. Chem. Phys. 164, 174710 (2026)
https://doi.org/10.1063/5.0324856

View Online
Export Citation

Articles You May Be Interested In

Rubber wear: Experiment and theory
J. Chem. Phys. (February 2025)

Sliding friction on ice
J. Chem. Phys. (May 2023)

A story of two transitions: From adhesive to abrasive wear and from ductile to brittle regime
J. Chem. Phys. (January 2024)

AIP Publishing

22 July 2026 11:10:36

The Journal of Chemical Physics | ARTICLE | pubs.aip.org/aip/jcp

Role of transfer films and interfacial cracking in metallic sliding wear

Cite as: J. Chem. Phys. 164, 174710 (2026); doi: 10.1063/5.0324856
Submitted: 27 January 2026 • Accepted: 20 April 2026 •
Published Online: 5 May 2026

View Online Export Citation CrossMark

R. Xu[1,2,3,a] and B. N. J. Persson[1,2,3]

AFFILIATIONS

[1] Peter Grünberg Institute (PGI-1), Forschungszentrum Jülich, 52425 Jülich, Germany
[2] State Key Laboratory of Solid Lubrication, Lanzhou Institute of Chemical Physics, Chinese Academy of Sciences, 730000 Lanzhou, China
[3] MultiscaleConsulting, Wolfshovener Str. 2, 52428 Jülich, Germany

Note: This paper is part of the 2026 JCP Emerging Investigators Special Collection.
[a] **Author to whom correspondence should be addressed:** r.xu@fz-juelich.de

ABSTRACT

The origin of wear particles in metallic sliding contacts remains debated. Classical views based on cold-welded junctions suggest that plastic yielding in the real contact area should lead to large wear coefficients, in apparent contradiction with the small values typically measured for metals. Here, we argue that this discrepancy can be resolved if most junctions do not directly produce wear particles but instead cause material transfer and the formation of a weakly bound transfer film. Wear then occurs intermittently when fragments of this film detach due to crack propagation at the interface between the transfer film and the underlying bulk metal. We performed unlubricated reciprocating sliding experiments on nominally smooth stainless steel, brass, and aluminum. For steel on steel, the wear mass loss shows an initial stage with negligible mass change up to a sliding distance of ~2.4 m, followed by a nearly linear regime, while the friction coefficient changes much less over the same sliding-distance range. For dissimilar-metal contacts, transfer-film formation is evidenced by optical imaging, net mass gain of the steel slider, and energy-dispersive x-ray spectroscopy. The results also show strongly asymmetric wear for some dissimilar-metal pairs. In addition, the collected wear debris is flake-like. These observations support a transfer-film-controlled wear mechanism associated with cold-welded junctions.

© 2026 Author(s). All article content, except where otherwise noted, is licensed under a Creative Commons Attribution (CC BY) license (https://creativecommons.org/licenses/by/4.0/). https://doi.org/10.1063/5.0324856

22 July 2026 11:10:36

I. INTRODUCTION

In the classical book on friction and lubrication, Bowden and Tabor[1] presented a theory for the friction between metals based on the formation and shearing of cold-welded junctions. They assumed that when two metallic blocks are squeezed together with a normal force F_N, the contact occurs only in a small fraction of the nominal contact area, where asperities make contact. They further assumed that the local stress in the contact regions is sufficiently large to plastically deform the metals. For unlubricated metals, the oxide and contamination films that are present on most metals in the normal atmosphere are broken or penetrated in the contact regions, resulting in cold-welded junctions.

In 1986, Archard presented the following argument against the assumption that sliding contacts between metals yield plastically and form cold-welded junctions:[2] Assume that each cold-welded junction results in the removal of a particle with a linear size comparable to the junction width d. If there are N junctions, then sliding a distance $L = d$ will generate N wear particles with volume $\Delta V \approx Nd^3$, so that

$$\frac{\Delta V}{L} \approx Nd^2.$$

If all contact has yielded plastically, then the real contact area is $A = Nd^2 = F_N/\sigma_P$, where σ_P is the penetration hardness, and one obtains

$$\frac{\Delta V}{L} = K\frac{F_N}{\sigma_P} \tag{1}$$

with $K \approx 1$. However, experiments for metals typically give $K \approx 10^{-6} - 10^{-3}$ (see Refs. 3–6), and Archard used this to argue that most contacts deform elastically rather than plastically, which would reduce the formation of cold-welded junctions. In this picture, K is interpreted as the probability that a contact results in a wear particle, but this in itself does not provide physical insight into the origin of the wear particles.

We argue that this conclusion is not compelling for nominally clean, unlubricated surfaces. Archard's argument relies on the key assumption that each junction produces a wear particle, which, in our view, is not the case. Most junctions formed in sliding contact do not directly generate wear debris. Instead, they primarily lead to metal transfer between the surfaces and to the formation of thin metallic films that are bound more weakly to the substrate than the bonding within the bulk metal. From time to time, flake-like fragments detach from this transfer film and form wear particles. Within this framework, there is no simple relation between the wear rate and the friction coefficient. Rather, the wear rate depends on additional factors, such as the bonding strength of the transfer films and the mechanisms by which fragments are removed from them.

This picture is related to the delamination theory of wear proposed by Suh[7] in 1973, where fatigue-driven nucleation and propagation of subsurface cracks eventually produce platelet-like debris, as illustrated in Fig. 1(a). This theory provides an important fracture-based picture of metallic wear, but it does not by itself explain all observations of metallic wear debris, as discussed below. Here, we propose that, instead of subsurface cracks, material removal occurs via crack propagation at the interface between the transfer layer and the underlying bulk metal, as illustrated in Fig. 1(b).

In this paper, we present reciprocating sliding experiments on several metallic systems to test this picture and to characterize the evolution of friction and wear in relation to transfer-film formation and removal.

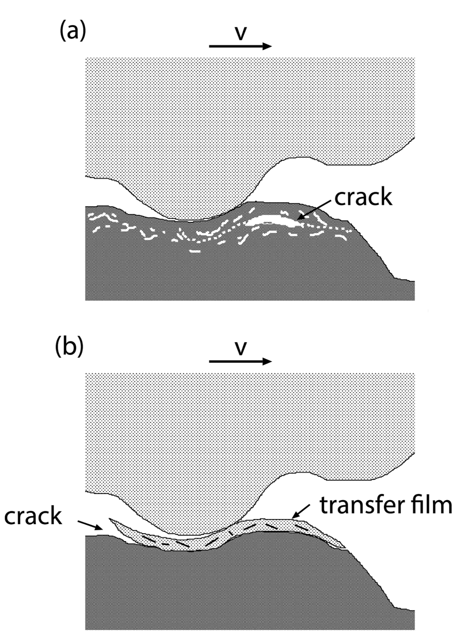

FIG. 1. Schematic illustration of two wear mechanisms in metallic sliding contacts. (a) Delamination-type wear, where subsurface crack nucleation and propagation lead to the formation of platelet-like debris. (b) Wear mechanism proposed in this study, where a weakly bound transfer film forms by metal transfer at cold-welded junctions, and crack propagation along the interface between the transfer film and the underlying bulk metal causes fragments of the film to detach.

II. EXPERIMENTS AND RESULTS

Specimen pairs made of various materials with nominally smooth surfaces were used. The materials included standard AISI 304 stainless steel; a two-phase H59 brass alloy composed of ~60 wt. % Cu and 40 wt. % Zn; and an AA 6061 aluminum alloy, a heat-treatable Al–Mg–Si alloy containing ~1.0 wt. % Mg and 0.6 wt. % Si. The upper specimen is referred to as the slider and the lower specimen as the substrate. The sliders were prepared as square blocks measuring 10×10 mm^2 with a thickness of 3 mm. Chamfers of 1 mm were made on all four edges to minimize edge effects during sliding, resulting in a nominal contact area of 8×8 mm^2. The substrates were flat plates with dimensions of 200×100 mm^2.

Linear reciprocating sliding tests were conducted using a custom-built machine. Each sliding cycle consisted of one forward and one backward motion of 120 mm at room temperature (≈30°C). The sliding speed was fixed at 1 mm s^{-1} to minimize frictional heating. The load was fixed at 180 N, resulting in a nominal contact pressure of 2.8 MPa. Between test cycles, the slider and substrate were cleaned with anhydrous ethanol and nonwoven fabric to remove wear debris and contaminants. Each test cycle was, therefore, considered to start from a clean surface.

During the experiments, the coefficient of friction and the wear rate of the slider were measured. The coefficient of friction was recorded directly by the machine. Mass loss was measured using a high-precision electronic balance (Huazhi PTX) with an accuracy of 0.1 mg.

For a steel-on-steel contact, Fig. 2 shows (a) the wear mass loss and (b) the friction coefficient as a function of sliding distance. During the first 2.4 m, there is negligible wear. After 2.4 m, the mass loss increases nearly linearly with the sliding distance. In this linear regime, Eq. (1) is obeyed with $K \approx 5 \times 10^{-3}$, where we have used the penetration hardness for steel, $\sigma_P = 6$ GPa.

Figure 2(a) shows that, for sliding distances >2.4 m, the wear mass is approximately proportional to the sliding distance, independent of the sliding distance between successive removals of wear particles. This differs from our earlier studies of granite on granite,[8] where the wear rate strongly decreases with increasing sliding distance as a considerable number of wear particles accumulate in the contact.

Figure 2(b) shows that the friction coefficient remains nearly constant up to a sliding distance of 7.2 m. For sliding distances longer than 12 m, the friction coefficient remains constant at ~0.7 (results not shown). We also observed that after a sliding distance of 12 m, the surface roughness power spectrum[9] no longer changes, indicating that the run-in distance for the steel-on-steel system is ~12 m. The other metal systems studied show a similar run-in distance.

For sliding between identical-metal pairs, material transfer is difficult to observe directly, but for dissimilar-metal pairs, it can be detected using energy-dispersive x-ray spectroscopy (EDS). The

22 July 2026 11:10:36

© Author(s) 2026

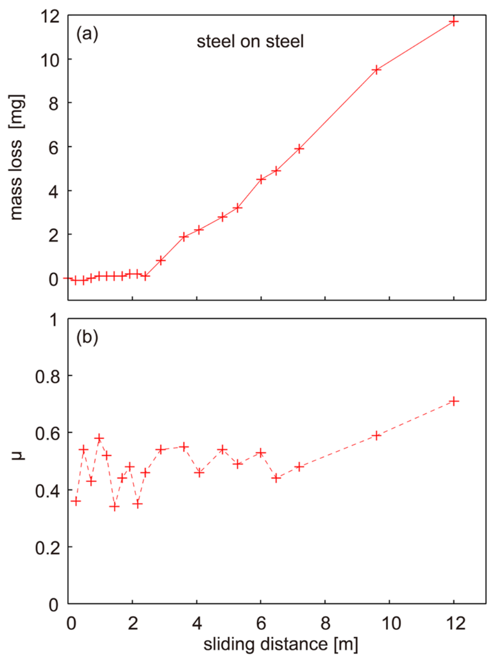

FIG. 2. (a) Mass loss and (b) friction coefficient as functions of sliding distance for a steel-on-steel contact. The data correspond to smooth-on-smooth surfaces tested at a nominal contact pressure of 2.8 MPa.

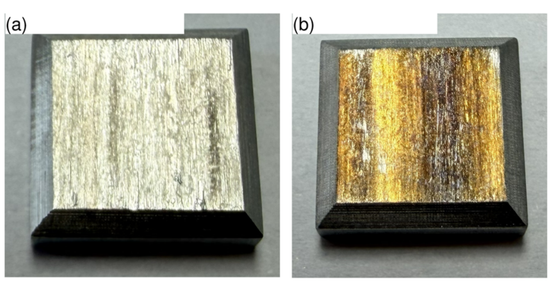

FIG. 3. Optical images of a steel slider after sliding 64.8 m on (a) an aluminum substrate and (b) a brass substrate. For steel sliding on brass, the transfer film appears as yellow regions on the steel surface.

EDS results show that metal transfer occurs between the steel slider and the aluminum and brass substrates (see Appendix A). In some cases, this transfer can also be seen in optical images, as shown in Fig. 3(b), where a yellow layer of brass builds up on the steel surface, and the dark regions may correspond to an oxide layer (e.g., ZnO).[10,11]

This transfer is also reflected in the slider mass change. After a sliding distance of 64.8 m, the steel slider mass increased by 0.7 mg for steel sliding on brass and by 0.5 mg for steel sliding on aluminum. For aluminum and brass sliding against each other, a decrease in mass is observed; however, strongly asymmetric wear is seen for these pairs (see Appendix B), where the wear rate of aluminum on brass is significantly higher than that of brass on aluminum. The dependence of wear on nominal contact pressure and the initial roughness combination was also studied for steel, brass, and aluminum sliding on steel (see also Appendix B). For these cases, the wear shows no obvious dependence on the initial roughness combination but tends to decrease with increasing nominal contact pressure.

Wear particles collected from the substrate in identical-metal pairs were studied using scanning electron microscopy (SEM). In all cases, we observe flake-like wear particles despite the obvious differences in particle size. This is shown in Fig. 4 for (a) steel on steel, (b) brass on brass, and (c) aluminum on aluminum.

III. DISCUSSION

The results reported above indicate that material transfer and the subsequent evolution of a transfer film play a central role in the present unlubricated experiments. For steel on steel, the wear mass loss exhibits an initial stage with negligible net mass change, followed by a regime of approximately linear mass loss, while the friction coefficient varies much less over the same sliding-distance range (Fig. 2). For dissimilar-metal pairs, transfer films are directly evidenced by optical imaging for steel sliding on brass (Fig. 3) and confirmed by EDS for steel sliding on aluminum and brass. The net mass gain of the steel slider provides quantitative evidence for material transfer to the steel surface and indicates that, after run-in, mass is added and removed at approximately equal rates so that wear occurs mainly between the transfer film and a counter surface covered by the same material. As a result, the total mass of the sliding block remains almost unchanged. To illustrate the asymmetric wear rates for brass and aluminum sliding against each other, we schematically show the corresponding asymmetric mass-transfer and wear mechanism in Fig. 5.

In another study, to be reported elsewhere, we found that the topography of a given sliding pair after run-in is similar regardless of the initial roughness. This is consistent with the weak dependence of wear rate on the three initial roughness combinations shown in Fig. 10, although the wear behavior during the run-in stage may still be affected by the initial roughness.

The fact that the wear rate after run-in is independent of the sliding distance suggests that, for steel sliding on steel under the present conditions, wear particles on the track do not continuously enter and accumulate in the contact region between the steel block and the substrate. Instead, they are removed efficiently from the sliding interface so that their concentration remains at an approximately steady level.

As for the trend that the wear rate decreases with increasing nominal contact pressure (see Appendix B), contact mechanics theory predicts that the real contact area is proportional to the load. Increasing the load mainly increases the number of macroasperity contacts in proportion to the load, and one would, therefore, expect the wear rate, when normalized by the normal force, to be independent of the load or nominal contact pressure. However, we find that it decreases with increasing load.

We attribute this to wear particles temporarily trapped at the sliding interface. As the normal force increases, both the contact area and the generation of wear particles increase. Thus, the concentration of wear particles at the sliding interface also increases. This, in turn, increases the surface separation and reduces the normalized

22 July 2026 11:10:36

© Author(s) 2026

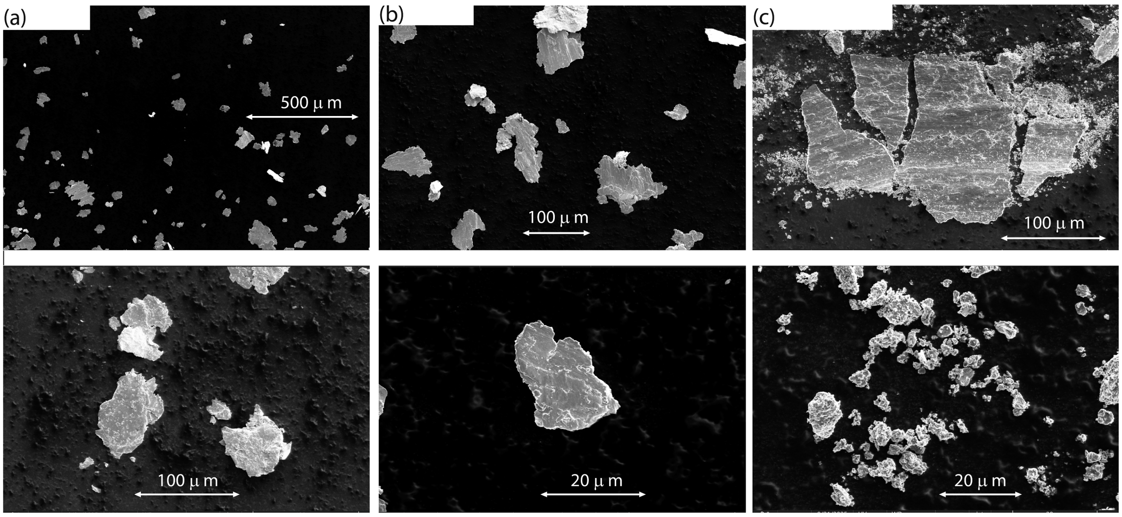

FIG. 4. Scanning electron microscopy (SEM) images of wear particles collected from the substrate for identical-metal sliding contacts: (a) steel on steel, (b) brass on brass, and (c) aluminum on aluminum. In all cases, the wear particles are flake-like, with lateral dimensions ranging from a few micrometers up to ∼100 μm.

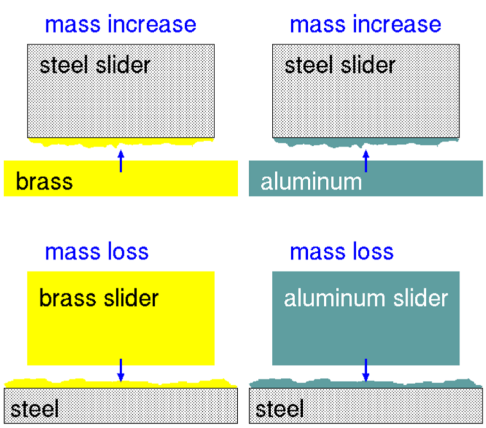

FIG. 5. Schematic illustration of two types of mass change after run-in. When a steel block slides on brass or aluminum, material is transferred from the substrate track to the steel block, and the mass of the steel block after run-in is greater than at the start. When a brass or aluminum block slides on steel, the mass loss of the sliding block increases linearly with sliding distance after run-in.

wear rate. A similar effect was observed for granite sliding on granite, where the wear rate decreased as wear particles accumulated at the sliding interface.[8]

Taken together, these observations support a picture in which wear is governed by the formation and intermittent removal of fragments from a weakly bound transfer film rather than by the friction coefficient alone. The flake-like debris collected for all identical-metal contacts studied (Fig. 4) also supports this mechanism. In addition, the wear process can be highly asymmetric depending on the material combination.

It is interesting to compare the results of our study with the fretting-wear study of Kirk *et al.*[12] They investigated wear for steel in contact with steel when the two surfaces undergo small-amplitude relative oscillatory motion (fretting). Since the oscillation amplitude is typically smaller than the linear size of the contact regions, and wear particles may remain between the surfaces for a long time before being ejected. They observed a thin, highly oxidized film (debris bed) at the interface and wear particles break off from this film, which is similar to the wear picture suggested by our study. Kirk *et al.* suggested that the thin film results from the agglomeration of wear particles via a sintering process, but the formation of the film must also involve metal transfer resulting from cold-welded junctions. The main difference may be that, while the wear particles in our study remain in the contact region between the solids only for a short time, in fretting wear, they may remain there for a long time and may repeatedly bind to and break off from the transfer film. As a result, the wear particles in fretting are highly oxidized.

The transfer of material from one surface to another during sliding has been the subject of numerous studies.[5] By the late 1940s, radioactive isotopes had become more readily available to researchers, making it possible to study material-transfer processes in the wear of metals. These techniques were applied by Rabinowicz[13] in his studies of metal wear. He presented a wear model for metals in which wear particles are removed when the elastic deformation energy stored in asperity contact regions becomes larger than the energy needed to break the bonds between the particle and the surrounding material, as illustrated in Fig. 6. In this model, wear-particle formation is due to crack propagation, and the energetic condition used by Rabinowicz is similar to the fracture criterion formulated by Griffith.[14]

One important implication of the Rabinowicz theory is that, if the frictional shear stress (or the kinetic friction coefficient) is small enough, there may not be sufficient elastic energy to form wear particles. Hence, a boundary lubrication film can have a large influence on the wear rate by reducing the frictional shear stress to such a degree that insufficient elastic energy is available to form wear

22 July 2026 11:10:36

© Author(s) 2026

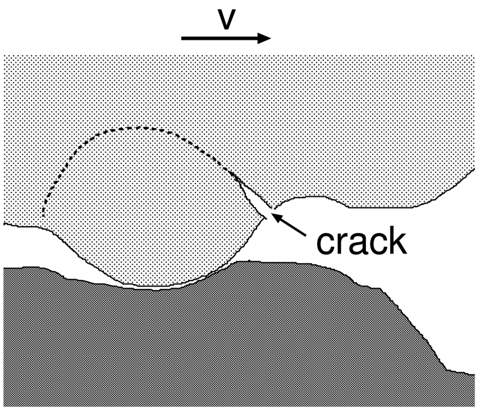

FIG. 6. Energetic criterion for the formation of wear particles in asperity contacts. To remove a particle of linear size d, sufficient elastic deformation energy must be stored in its vicinity to break the bonds required to form a free particle. The bond-breaking energy scales as $U_c \approx \gamma d^2$, where γ is the cohesive energy per unit surface area, while the elastic energy scales as $U_{el} \approx (\tau^2/E)d^3$, where τ is the shear stress in the asperity contact region. Hence, particle removal is possible only if $d > \gamma E/\tau^2$, so only sufficiently large asperity contact regions give rise to wear particles.

particles. In this model, a strong dependence of wear rate on the sliding friction coefficient is expected, as was indeed observed by Rabinowicz in a large set of experiments, where low wear rates and low friction occurred for lubricated contacts.[6] In the present experiments, however, measurable wear for steel on steel appears only after an initial sliding stage, while the friction coefficient changes much less over the same sliding-distance range. This suggests that, under the present conditions, wear is controlled primarily by the formation and detachment of a weakly bound transfer film, rather than by a direct one-to-one relation between wear rate and friction coefficient.

The Rabinowicz-type energy criterion and related fracture-based removal mechanisms may be most relevant in the initial stage of wear for metals with very large roughness, and they may also apply to some brittle nonmetals and rubber-like materials.[15–17] For most nominally clean, unlubricated metallic surfaces, we suggest that the dominant wear mechanism involves fragments removed from weakly bound transfer films formed by metal transfer between the two sliding bodies due to cold-welded junctions. However, we cannot exclude the possibility that wear may also occur through the delamination mechanism proposed by Suh,[7] since in that case, some initial sliding distance without measurable wear may also be required to build up the defect concentration in the subsurface. Nevertheless, this mechanism does not by itself naturally explain why the wear debris is often highly oxidized,[10–12] whereas such oxidation is more readily understood within the wear mechanism we propose.

Molinari and co-workers have used molecular dynamics to study wear between sliding solids with plasticity.[18,19] In the simulations, wear particles form if the elastic deformation energy is larger than the energy required to form a free particle. If this is not the case, plastic smoothing of the asperities is observed. However, the wear particles tend to be roughly spherical, which differs from the flake-like particles we observe. In addition, for rough surfaces, wear starts immediately upon sliding, whereas for steel on steel, we observe an initial sliding period without wear, which we associate with the build-up of weakly attached transfer films. It would be interesting to extend these molecular dynamics studies by including oxide or contamination films on the metallic bodies.

IV. SUMMARY AND CONCLUSION

We have investigated unlubricated reciprocating sliding for several metallic systems with nominally smooth surfaces, focusing on the relation among friction, wear, and material transfer. For steel on steel, the wear mass loss exhibits an initial stage with negligible mass change up to a sliding distance of ~2.4 m, followed by a nearly linear increase. Over the same sliding-distance range, the friction coefficient changes much less, indicating that, under the present conditions, the wear rate is not determined by the friction coefficient alone.

For dissimilar-metal contacts, material transfer is directly evidenced by optical images for steel sliding on brass and confirmed by EDS and by the mass change, especially the net mass gain of the steel slider on brass and aluminum substrates. Finally, SEM observations show that the wear debris is flake-like for the identical-metal contacts.

Based on these results, we propose that unlubricated metallic wear is a two-step process. First, metal transfer at cold-welded junctions forms a weakly bound transfer film. Second, when the transfer film becomes sufficiently developed, crack propagation at the interface between the transfer film and the underlying bulk metal leads to partial detachment of the film and the formation of flake-like wear particles. This mechanism is distinct from subsurface delamination and provides a physical interpretation of why small wear coefficients can coexist with junction formation in nominally clean metallic contacts. Overall, the present results indicate that wear is governed primarily by the formation, evolution, and intermittent removal of transfer films and that material transfer can lead to highly asymmetric wear behavior.

ACKNOWLEDGMENTS

We thank H. Ren (LICP, CAS, Lanzhou 730000, China) for the help with the SEM and EDS experiments.

AUTHOR DECLARATIONS

Conflict of Interest

The authors have no conflicts to disclose.

Author Contributions

R. Xu: Conceptualization (equal); Data curation (equal); Formal analysis (equal); Funding acquisition (equal); Investigation (equal); Methodology (equal); Project administration (equal); Resources (equal); Software (equal); Supervision (equal); Validation (equal); Visualization (equal); Writing – original draft (equal); Writing – review & editing (equal). **B. N. J. Persson**: Conceptualization (equal); Data curation (equal); Formal analysis (equal); Funding acquisition (equal); Investigation (equal); Methodology (equal);

22 July 2026 11:10:36

© Author(s) 2026

Project administration (equal); Resources (equal); Software (equal); Supervision (equal); Validation (equal); Visualization (equal); Writing – original draft (equal); Writing – review & editing (equal).

DATA AVAILABILITY

The data supporting the findings of this study are available from the corresponding author upon reasonable request.

APPENDIX A: POST-TEST SURFACE MORPHOLOGY AND EDS ELEMENTAL MAPPING

Figure 7 shows the post-test appearance of selected metal sliders tested under the nominal conditions used in this study on different substrates. The first column shows the optical photographs of the slider surfaces. For some material combinations, clear color variations can be observed, indicating the presence of transferred material on the slider surface.

Figure 7 also shows the surface images and elemental maps obtained using a Quanta 650 FEG equipped with energy-dispersive x-ray spectroscopy (EDS). The second column shows the corresponding electron micrograph. The third column shows the elemental signal corresponding to the slider material, and the remaining columns show the elemental signals corresponding to elements from the substrate.

For all material combinations shown, elements originating from the substrate are detected on the slider surface. This confirms that interfacial material transfer occurred during sliding. The relative intensity and spatial distribution of these signals indicate that the extent of transfer differs among the tested material pairs.

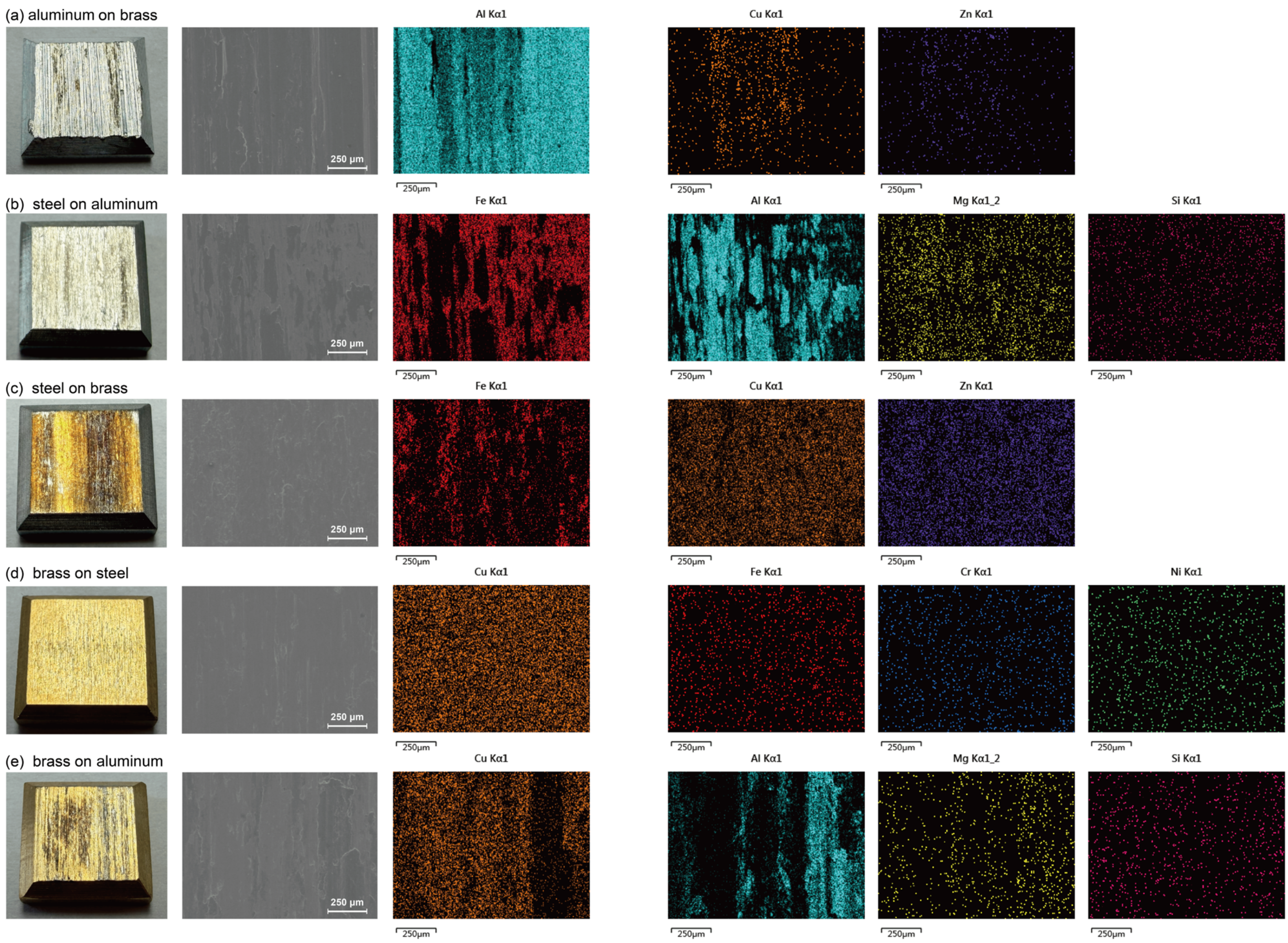

FIG. 7. Post-test appearance and EDS elemental maps of selected metal sliders tested under the nominal conditions used in this study. For each material combination, the first image shows the optical photograph of the slider surface, the second image shows the corresponding electron micrograph, the third image shows the elemental signal of the slider material, and the remaining images show the elemental signals of the substrate. In all cases, elements originating from the substrate are detected on the slider surface, confirming that material transfer occurred during sliding. The distribution and intensity of the transferred elements vary among the different material pairs. (a) Aluminum on brass, (b) steel on aluminum, (c) steel on brass, (d) brass on steel, and (e) brass on aluminum.

22 July 2026 11:10:36

© Author(s) 2026

APPENDIX B: WEAR OF IDENTICAL AND DISSIMILAR METAL PAIRS AND DEPENDENCE ON NOMINAL CONTACT PRESSURE AND INITIAL ROUGHNESS COMBINATIONS

Figure 8 shows the mass loss as a function of sliding distance for two steel-on-steel tests performed under the same nominal conditions. The red plus symbols reproduce the data shown in Fig. 2, while the blue cross symbols correspond to another test carried out over a longer total sliding distance. In both cases, after an initial stage with negligible wear, the mass loss increases approximately linearly with sliding distance. The fitted slopes are ~1.1 and 2.17 mg/m, corresponding to normalized wear rates of ~0.006 and 0.012 mg/Nm, respectively.

The fitted slopes indicate different wear rates for the two tests. One possible reason is that the experiments were performed under different environmental conditions: The red data were obtained during winter, whereas the blue data were obtained during summer, with the sliding equipment located in a room without temperature regulation. The temperature was ~30 °C in summer and ~0 °C in winter. Hence, the difference in wear rates may reflect differences in temperature and humidity.

Figure 9 shows the wear rates after run-in for combinations of three metal slider–substrate pairs. The filled symbols correspond to the identical-metal pairs, and the open symbols correspond to the dissimilar brass–aluminum pairs.

The wear rate is the highest for steel on steel and very low for both aluminum on aluminum and brass on aluminum. In contrast, the wear rate for aluminum on brass is is comparable to that for brass on brass but much higher than those for brass on aluminum and aluminum on aluminum.

Figure 10 shows the wear rates after run-in for steel, aluminum, and brass sliding on steel substrates. We show results for different nominal contact pressures and for three initial surface roughness combinations of slider and substrate, namely, smooth–smooth, rough–smooth, and smooth–rough.

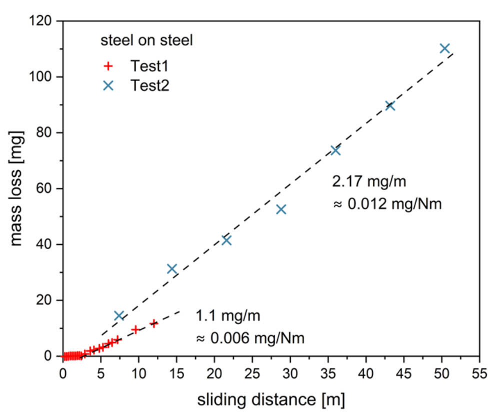

FIG. 8. Mass loss as a function of sliding distance for steel-on-steel contact. The red plus symbols reproduce the data shown in Fig. 2, while the blue cross symbols show the results from another test extending to a longer total sliding distance. The dashed lines indicate the approximately linear wear regimes for the two tests. In both cases, the measurements were performed for smooth-on-smooth pairs at a nominal contact pressure of 2.8 MPa.

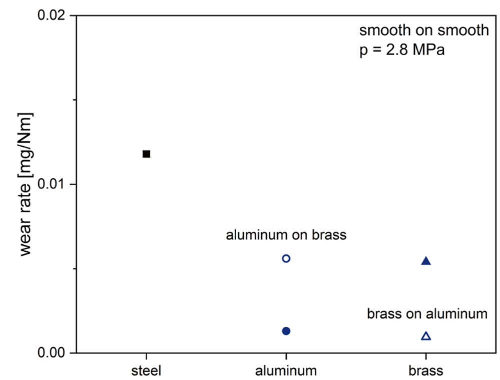

FIG. 9. Wear rates after run-in for three slider materials. The filled symbols correspond to identical-material pairs, the open circle corresponds to aluminum sliding on brass, and the open triangle corresponds to brass sliding on aluminum. In all cases, the measurements were performed for smooth-on-smooth pairs at a nominal contact pressure of 2.8 MPa.

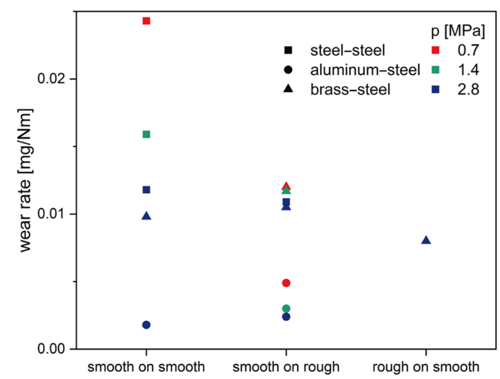

FIG. 10. Wear rates after run-in for three initial roughness configurations and three nominal contact pressures. The squares, circles, and triangles correspond to steel on steel, aluminum on steel, and brass on steel, respectively. The red, green, and blue symbols correspond to nominal contact pressures of 0.7, 1.4, and 2.8 MPa, respectively.

The wear rate for steel on steel is similar to that for brass on steel and higher than that for aluminum on steel, and the wear rates show no obvious dependence on the initial roughness combination and tend to decrease with increasing nominal contact pressure.

The very small wear rate for brass sliding on aluminum in Fig. 9 and for aluminum sliding on steel in Fig. 10 suggests that aluminum is transferred to the counter surface and forms a transfer film, after which sliding occurs mainly at an aluminum–aluminum interface, leading to a lower wear rate similar to that for aluminum on aluminum. For these cases, the removed fragments may consist mainly of transferred aluminum, although a small amount of brass or steel may also be involved. If only transferred aluminum were removed, the measured mass of the sliding block would be expected to remain nearly unchanged after run-in.

However, for aluminum sliding on brass, the wear rate is much higher than that for brass sliding on aluminum and also higher than

22 July 2026 11:10:36

© Author(s) 2026

that for aluminum sliding on steel. At present, we do not have a definitive explanation for this asymmetry. One possible reason is that brass is plastically harder than aluminum, and brass asperities may break the oxide coating on the aluminum surface more effectively, resulting in stronger formation of cold-welded junctions than in aluminum–aluminum contact.

REFERENCES

[1] F. P. Bowden and D. Tabor, *The Friction and Lubrication of Solids* (Oxford University Press, Oxford, 2001).
[2] J. F. Archard, "Friction between metal surfaces," Wear **113**, 3 (1986).
[3] J. F. Archard, "Contact and rubbing of flat surfaces," J. Appl. Phys. **24**, 981 (1953).
[4] J. F. Archard and W. Hirst, "The wear of metals under unlubricated conditions," Proc. R. Soc. London, Ser. A **236**, 397 (1956).
[5] J. A. Greenwood, "Metal transfer and wear," Front. Mech. Eng. **6**, 62 (2020).
[6] E. Rabinowicz, "The wear coefficient magnitude, scatter, uses," J. Lubr. Technol. **103**, 189 (1981).
[7] N. P. Suh, "The delamination theory of wear," Wear **25**, 111 (1973).
[8] S. Sukhomlinov, M. H. Müser, and B. N. J. Persson, "Granite sliding on granite: Friction, wear rates, surface topography, and the scale-dependence of rate-state effects," Rep. Prog. Phys. **89**, 038301 (2026).
[9] N. Rodriguez, L. Gontard, C. Ma, R. Xu, and B. N. J. Persson, "On how to determine surface roughness power spectra," Tribol. Lett. **73**, 18 (2025).
[10] M. Dienwiebel and K. Pöhlmann, "Nanoscale evolution of sliding metal surfaces during running-in," Tribol. Lett. **27**, 255 (2007).
[11] T. Feser, P. Stoyanov, F. Mohr, and M. Dienwiebel, "The running-in mechanisms of binary brass studied by in-situ topography measurements," Wear **303**, 465 (2013).
[12] A. M. Kirk, P. H. Shipway, W. Sun, and C. J. Bennett, "Debris development in fretting contacts—Debris particles and debris beds," Tribol. Int. **149**, 105592 (2020).
[13] E. Rabinowicz, *Friction and Wear of Materials* (John Wiley, New York, 1965), pp. 121–122.
[14] A. A. Griffith, "The phenomena of rupture and flow in solids," Philos. Trans. R. Soc. London, Ser. A **221**, 163 (1921).
[15] B. N. J. Persson, R. Xu, and N. Miyashita, "Rubber wear: Experiment and theory," J. Chem. Phys. **162**, 074704 (2025).
[16] R. Xu and B. N. J. Persson, "Sliding wear: Role of plasticity," Tribol. Lett. **73**, 109 (2025).
[17] R. Xu, N. Miyashita, and B. N. J. Persson, "Rubber wear on concrete: Dry and in-water conditions," Wear **578–579**, 206200 (2025).
[18] T. Brink and J.-F. Molinari, "Adhesive wear mechanisms in the presence of weak interfaces: Insights from an amorphous model system," Phys. Rev. Mater. **3**, 053604 (2019).
[19] R. Aghababaei, D. H. Warner, and J.-F. Molinari, "Critical length scale controls adhesive wear mechanisms," Nat. Commun. **7**, 11816 (2016).

22 July 2026 11:10:36

© Author(s) 2026